

Formation and micromachining of Teflon (fluorocarbon polymer) film by a completely dry process using synchrotron radiation

Muneto Inayoshi, Masafumi Ito, Masaru Hori, and Toshio Goto
Department of Quantum Engineering, Nagoya University, Chikusa, Nagoya 464-0814, Japan

Mineo Hiramatsu^{a)}
Department of Electrical and Electronic Engineering, Meijo University, Tempaku, Nagoya 468-8502, Japan

(Received 22 December 1998; accepted 12 March 1999)

The development of a new fabrication technique of Teflon microparts using synchrotron radiation (SR) irradiation, the SR ablation process, was described. The anisotropic micromachining and thin film formation of polytetrafluoroethylene, fluorinated ethylene propylene, and perfluoroalkoxy were demonstrated using the SR ablation process. The anisotropic micromachining of Teflon with hole pattern of 2 μm diam was successfully performed, and the micromachining of Teflon with a high aspect ratio of 50 was achieved. Moreover, Teflon films with flat surface were formed at a high rate by the SR ablation of Teflon at the substrate temperature above 200 °C. © 1999 American Vacuum Society. [S0734-211X(99)06803-1]

I. INTRODUCTION

Fluorocarbon polymer has excellent properties such as high electrical resistivity, low coefficient of friction, high thermal and chemical stability, low dielectric constant, potential biocompatibility, nonwetting property, and so on. Polytetrafluoroethylene (PTFE), fluorinated ethylene propylene (FEP), and perfluoroalkoxy (PFA), which are well known as "Teflon," are fluorocarbon polymers with excellent properties, and have attracted considerable attention for applications in various fields. For example, in the emerging field of microelectromechanical system, Teflon is potentially useful as the sliding material in the drive shafts of micromachines, soft structural material in microactuator, and in man-made internal organs. In order to realize these applications, development of techniques for the formation of Teflon thin films as well as the micromachining of Teflon with high aspect ratio (the ratio of the depth and the pattern width) is required.

So far, micromachining and formation of Teflon have been extensively attempted by the laser ablation technique using pulsed lasers such as the vacuum ultraviolet (VUV) pulsed laser and the ultrashort pulsed laser.¹ The absorption coefficient of Teflon is large in the VUV-UV range and VUV or UV lasers than infrared lasers which induce less thermal damage to the Teflon.² Although the Teflon was ablated at a high rate (a few microns per pulse) by the laser irradiation, the aspect ratio of the ablated Teflon was very low.³ Therefore, the pulsed laser ablation technique is not suitable for micromachining of Teflon with high aspect ratio.

On the other hand, synchrotron radiation (SR) is unique light with high intensity and high direction ability in the wavelength region from soft x ray to VUV. The use of SR potentially offers extremely important advantages over conventional UV laser processing due to its short wavelength, which enables us to realize a fabrication process of devices

with submicron features. So far, many investigations related to lithography, material processing, and LIGA (acronym for German words lithographie, galvanofornung, abfornung) have been pursued with SR.⁴ In the LIGA process, which consists of SR lithography of polymethylmethacrylate (PMMA) film and electric plating technique, the formation and micromachining processes of PMMA are performed by wet processes. If these wet processes are removed from the LIGA process, the micromachine fabrication process can be simple and performed at low cost and in a short period.

Recently, a few reports have been published on the micromachining of PTFE bulk employing SR. Zhang *et al.* have demonstrated the direct micromachining of PTFE bulk with a high aspect ratio using the ablation process by the SR-induced reaction, that is, the SR ablation process.⁵ Inayoshi *et al.* have demonstrated the direct micromachining of PTFE bulk as well as high-rate formation of PTFE thin films by using the SR ablation process.⁶ From the practical point of view, it is necessary to survey the several kinds of fluorocarbon polymer materials including PTFE for the application of the SR ablation process. The SR ablation process, which is a completely dry process, can be a key technology for the fabrication of microparts in micron size in the next generation. Moreover, the SR ablation process for the Teflon thin film formation utilizes a solid source as a starting material without using reactive gases such as fluorocarbon gases causing a serious environmental problem of global warming. Therefore, the SR ablation process is essentially clean compared with plasma polymerization or plasma-enhanced chemical vapor deposition methods. In order to establish a completely dry process consisting of thin film formation and high-aspect ratio micromachining of Teflon using the SR ablation process for the practical use, it is necessary to clarify the decomposition mechanism of Teflon by the SR-induced reaction as well as to optimize the process condition including variation of fluorocarbon polymer materials, wavelength of SR beam, photon flux or dose, which is defined as the

^{a)}Electronic mail: mnhrmt@meijo-u.ac.jp

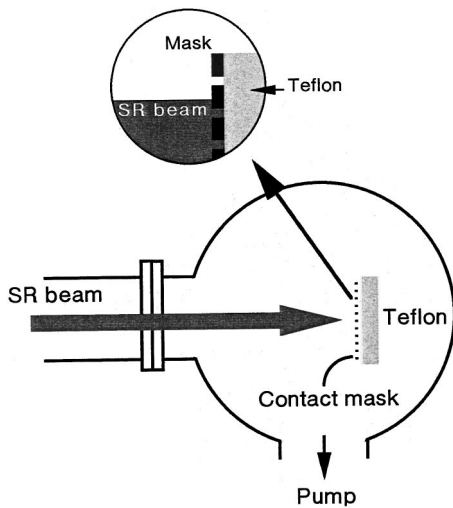


FIG. 1. Schematic diagram of experimental apparatus used to micromachining of Teflon by the SR ablation process.

product of SR irradiation time and the storage ring current, and so on.

In this article, we describe the Teflon fabrication technique as a completely dry process consisting of thin film formation and micromachining of Teflon. The anisotropic micromachining and thin film formation of three types of Teflon materials, PTFE, FEP, and PFA, are systematically demonstrated using the SR ablation process.

II. EXPERIMENTS

The experiments were carried out using beamline 8A (BL-8A) at UVSOR at the Institute for Molecular Science, Okazaki National Research Institute, Japan. The wavelength region of SR beam spanned 0.4–800 nm. The peak in the spectrum of this beam corresponds to the wavelength region around 10 nm.

Figure 1 shows a schematic diagram of the experimental apparatus used for micromachining of Teflon by the SR ablation process. This system consists of the SR beam, a reaction chamber, and a pumping system. The reaction chamber was evacuated to 1.3×10^{-1} Pa using a turbomolecular pump backed by a rotary pump before irradiation of SR beam. The Teflon targets were set perpendicularly to the SR beam. PTFE, PFA, and FEP were employed as the targets. The chemical structure, molecular weight, and melting temperature of each target are summarized in Table I. A nickel (Ni) mesh (a square pattern of $77 \mu\text{m}$), a copper (Cu) mesh (a square pattern of $19 \mu\text{m}$), and a capillary plate made of plumbum-containing glass (Pb-SiO_2) with capillaries of $2 \mu\text{m}$ inner diameter were used for the contact mask. Direct writing in Teflon using the SR ablation was carried out at room temperature.

The cross section of Teflon targets ablated by SR irradiation was observed using a scanning electron microscope (SEM). The depth of Teflon target ablated by SR irradiation was measured from the cross sectional SEM photograph. Before SEM observation, a conductive metal of osmium was coated on the sample using a plasma coater (NL OPC80,

TABLE I. Structure, molecular weight, and melting temperature of each target.

Material	Structure				Molecular weight	Melting temperature
PTFE Polytetrafluoroethylene	F	F	F	F	10^7 g/mol	327°C
	- C -	- C -	- C -	- C -		
	F	F	F	F		
PFA Perfluoroalkoxy	F	F	F	F	10^6 g/mol	305°C
	- C -	- C -	- C -	- C -		
	F	O	F	F		
		C_3F_7				
FEP Fluorinated ethylene propylene	F	F	F	F	10^5 g/mol	260°C
	- C -	- C -	- C -	- C -		
	F	CF_3	F	F		

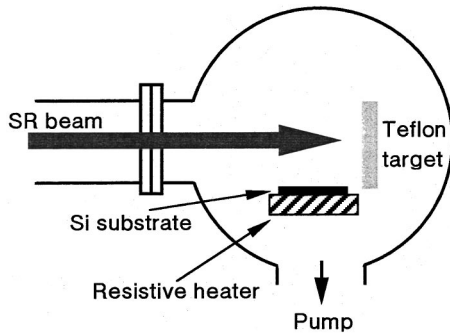


FIG. 2. Schematic diagram of experimental apparatus used for film formation of Teflon by the SR ablation process.

Nippon Laser and Electronics Laboratory) in order to enhance the secondary electron emission efficiency.⁷

Figure 2 shows a schematic diagram of the experimental apparatus used for the thin film formation of Teflon by the SR ablation process. The reaction chamber was common to both experiments of micromachining and film formation of Teflon. The Teflon bulk as a target and silicon (Si) (100) substrate were set perpendicularly and parallel to the SR beam, respectively. The distance between the surface of the Si substrate and the SR beam was 1 cm. The film formation of Teflon using the SR ablation process was carried out with the variation of substrate temperature in the range from 25 to 300 °C. The substrate temperature was chosen so as not to exceed the melting temperature of each Teflon target. The resistive heater was used for heating the substrate. The substrate temperature was monitored using a thermocouple in contact with the surface of the substrate. The deposition rate was evaluated by measuring a film thickness using a tally step. The films deposited by the SR ablation process were analyzed by Fourier transform infrared spectroscopy (FTIR) and x-ray photoelectron spectroscopy (XPS).

III. RESULTS AND DISCUSSION

A. Micromachining of Teflon using SR ablation process

Teflon was ablated by the SR irradiation effectively in the vacuum. Figure 3 shows the SEM image of SR-ablated pattern created in a PTFE sheet of 1 mm thickness. As seen in Fig. 3, the fine pattern of 77 μm square holes was successfully produced in the PTFE sheet by the irradiation of the SR beam. The pattern created in the back side of the PTFE sheet penetrated by the SR ablation was found to be almost the same as the fine pattern of the front side shown in Fig. 3. Therefore, the anisotropic ablation of PTFE with an aspect ratio of ten was successfully achieved by the SR ablation process. Figure 4 shows a cross sectional SEM image of a PTFE sheet of 5 mm thickness with 77 μm square-hole pattern produced by the SR ablation process. As seen in Fig. 4, 77 μm square holes were bored completely in the thick PTFE sheet. As a result, the anisotropic ablation of PTFE at an aspect ratio of 50 was achieved by the SR ablation process. Although the lines of a few microns width were ob-

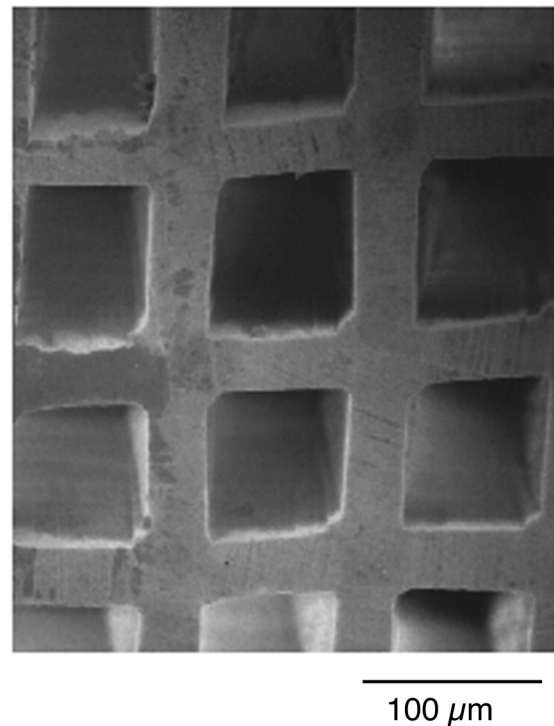


FIG. 3. SEM photograph of fine pattern with 77 μm square holes created in PTFE by the SR ablation process.

served in the side wall of PTFE ablated by the SR irradiation as seen in Fig. 4, the size of these lines was the same as the surface roughness of Ni mask. In addition, anisotropic micromachining of FEP and PFA with 19 μm square-hole pat-

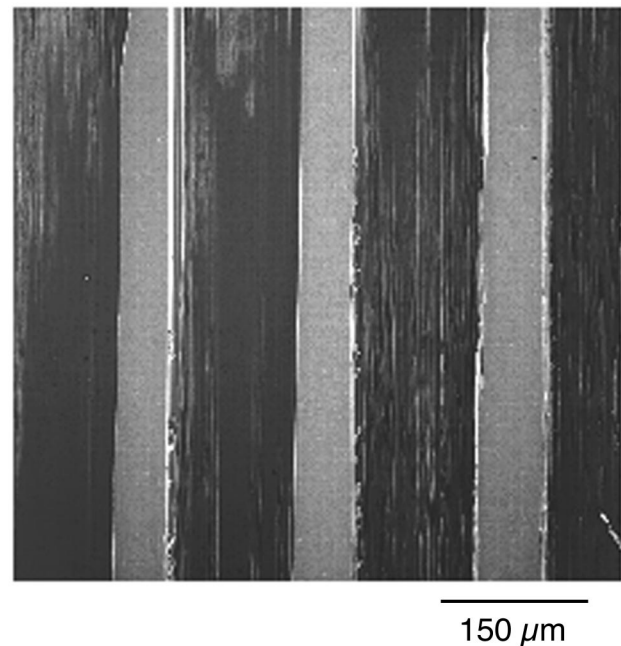


FIG. 4. Cross sectional SEM image of PTFE fine pattern with 77 μm square holes created in PTFE created by the SR ablation process.

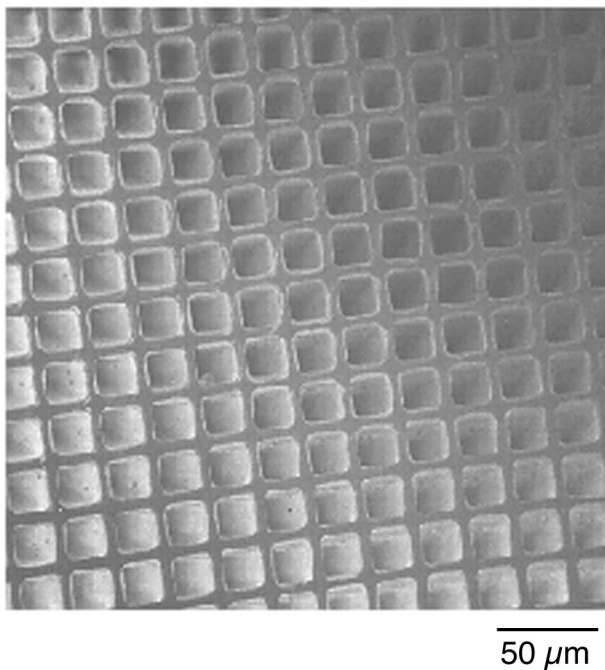


FIG. 5. SEM photograph of fine pattern with 19 μm square holes created in FEP by the SR ablation process.

tern was also realized successfully for the first time (Fig. 5). Figure 6 shows the SEM image of 2 μm hole pattern created in a PTFE sheet by the SR irradiation. A capillary plate of Pb-SiO₂ with capillaries of 2 μm inner diameter was used as

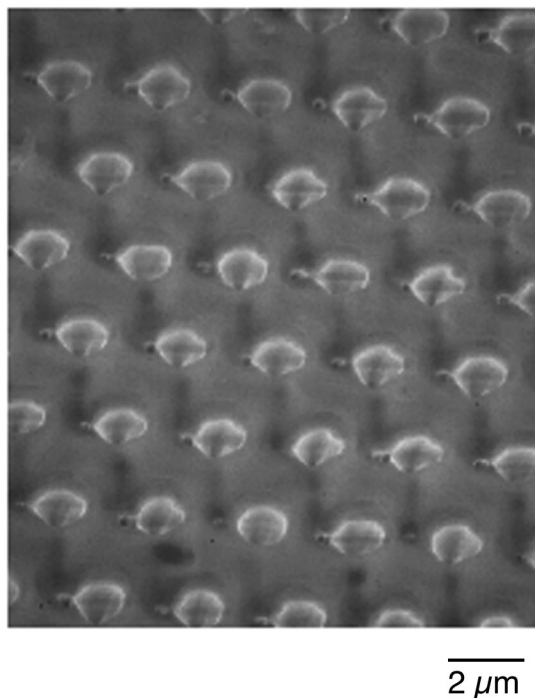


FIG. 6. SEM photograph of fine pattern with 2 μm holes created in PTFE by the SR ablation process.

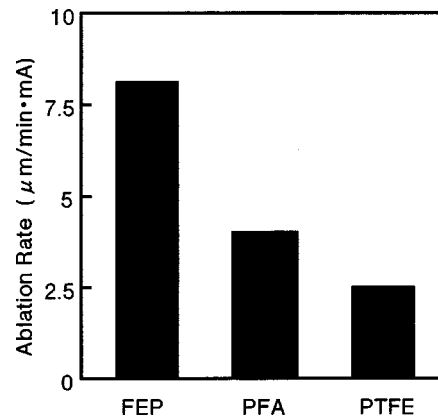


FIG. 7. Ablation rates of PTFE, PFA, and FEP in the case using a Ni mask with a 77 μm square-hole pattern.

a contact mask. As seen in Fig. 6, the fine pattern of 2- μm -diam holes was developed using the SR ablation process. It must be pointed out that the mask pattern of the capillary plate was distorted due to the heating of the Pb-SiO₂ material caused by the SR absorption. The created fine pattern shown in Fig. 6 closely followed the distorted mask pattern. Consequently, the micromachining of Teflon in micron unit with high precision was realized.

Figure 7 shows the ablation rates of the PTFE, PFA, and FEP in the case using Ni contact mask with 77 μm square-hole pattern at room temperature. The ablation rate was normalized by dose. As seen in Fig. 7, PTFE was ablated at a high rate of 2.5 $\mu\text{m}/\text{min}\cdot\text{mA}$ by the SR irradiation, corresponding to the ablation rate of 400 $\mu\text{m}/\text{min}$ for the typical ring current of 160 mA, which was very high from a practical point of view. The ablation rate for FEP, which has the lowest molecular weight and melting temperature among three types of materials investigated, was higher than the ablation rates for PFA and PTFE. Results in Fig. 7 indicate that fluorocarbon polymers with the lower molecular weight are more easily ablated by the SR irradiation. The decomposition of fluorocarbon polymers through the SR-induced reaction into the volatile fragments would proceed until the molecular weight of the decomposed fragments became small enough to be removed from the polymer surface into the vacuum. Indeed, from *in situ* quadruple mass spectroscopy (QMS) analysis of gaseous products generated by the SR ablation of Teflon, strong ion signal intensities of C (12 amu), F (19 amu), CF (31 amu), CF₂ (50 amu), and CF₃ (69 amu) were observed. Moreover, ion signals of the fragments with the mass more than 300 amu were contained in the mass distribution of the gaseous products generated from each target irradiated by SR beam.

B. Formation of fluorocarbon film using SR ablation process

Formation of Teflon films using the SR ablation process was also demonstrated. A Teflon target was ablated by the SR irradiation and the thin films of Teflon were deposited on the Si (100) substrate placed normal to the target surface as

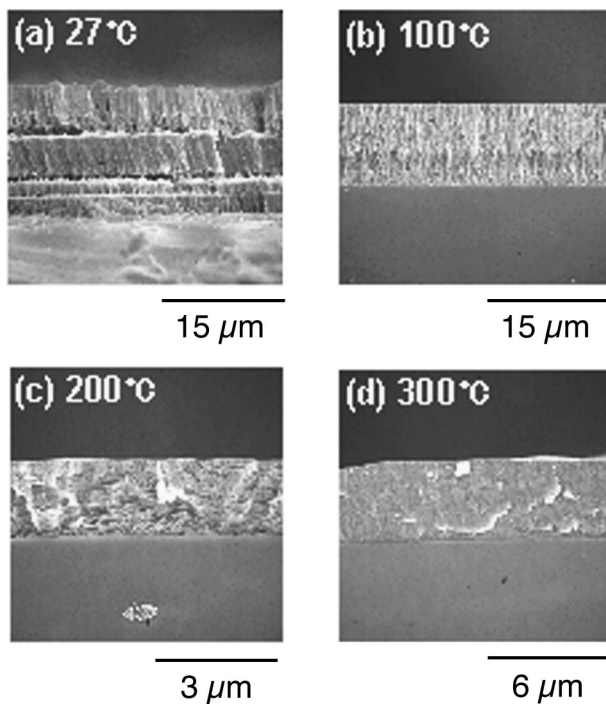


FIG. 8. Cross sectional SEM images of PTFE films formed at substrate temperatures of (a) 27 °C, (b) 100 °C, (c) 200 °C, and (d) 300 °C by the SR ablation process.

shown in Fig. 2. Figures 8–10 show the cross sectional SEM photographs of PTFE, PFA, and FEP films formed by the SR ablation process at substrate temperatures of (a) 27 °C, (b) 100 °C, (c) 200 °C, and (d) 300 °C. The films deposited at

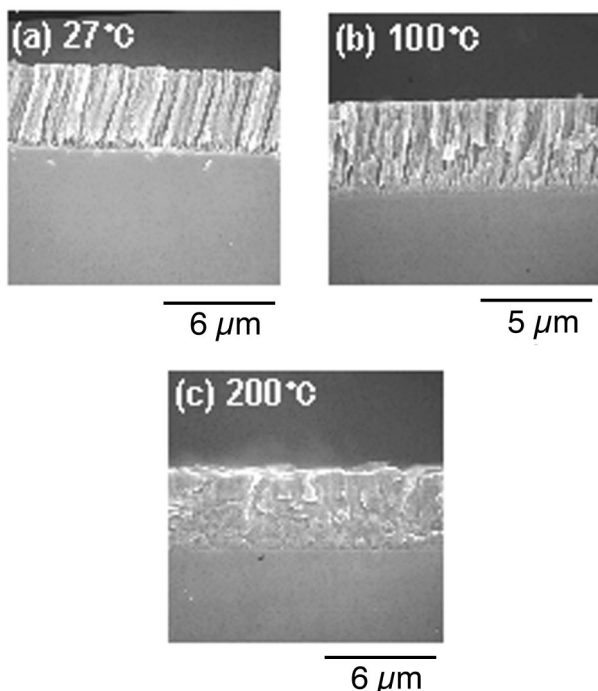


FIG. 9. Cross sectional SEM images of PFA films formed at substrate temperatures of (a) 27 °C, (b) 100 °C, and (c) 200 °C by the SR ablation process.

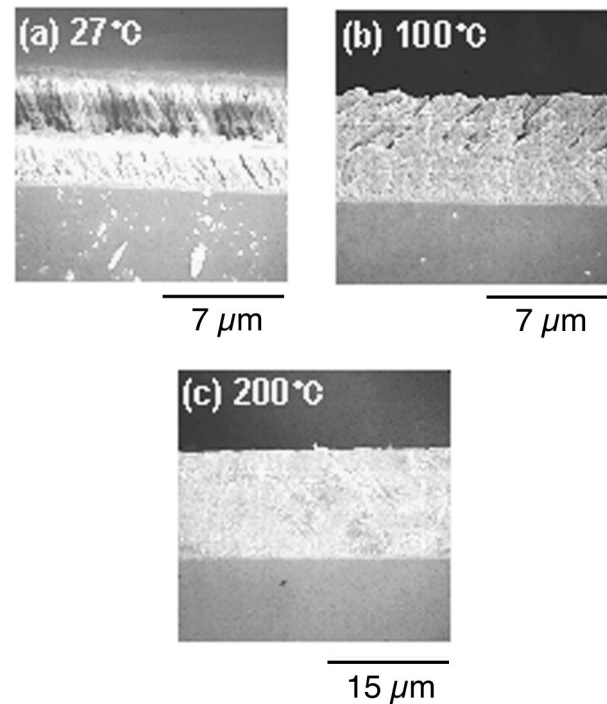


FIG. 10. Cross sectional SEM images of FEP films formed at substrate temperatures of (a) 27 °C, (b) 100 °C, and (c) 200 °C by the SR ablation process.

room temperature for all materials look like the bundle of the chemical fibers as shown in Figs. 8(a), 9(a), and 10(a), and the quality of these films was not good. As was stated previously from QMS measurement, in addition to major radicals such as CF_x ($x=1-3$), a certain number of fragments with large molecular weight more than 300 amu as oligomers would be produced from the surface of Teflon irradiated by SR beam. Since the repolymerization of the large fragments cannot proceed well on the substrate at low substrate temperature, the surface of the deposited film became very rough. On the other hand, the quality of the films improved with increasing substrate temperature, and high-quality films with smooth surface were formed on the Si substrate at the substrate temperature above 200 °C, which was just below the melting temperature of Teflon target used in the present study. This fact indicates that the fragments generated from the target surface by the SR ablation were repolymerized effectively on the substrate surface by heating.

Figure 11 shows the deposition rates of fluorocarbon films formed at the substrate temperature of 200 °C. The deposition rates of PTFE, PFA, and FEP were 15, 26, and 47 nm/min mA, respectively. The deposition rate of PTFE corresponds to the deposition rate of 2560 nm/min for a typical ring current of 160 mA. This value is an order of magnitude larger than that obtained using conventional plasma polymerization method. Furthermore, the deposition rate of FEP film was higher than those of PFA and PTFE films. The result in Fig. 11 indicates the usefulness of the SR-ablation process for the high-rate deposition of Teflon thin films. From the fact that the ablation rate of FEP was also higher than those of PFA and PTFE as seen in Fig. 7, the higher deposition

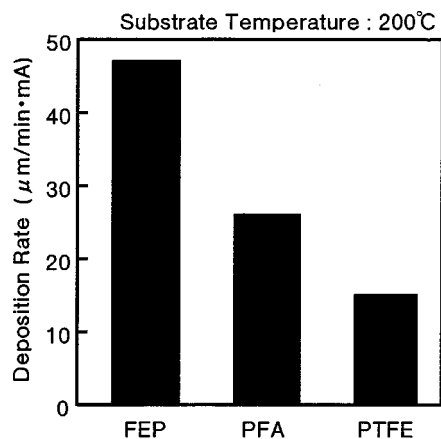


FIG. 11. Deposition rates of fluorocarbon films formed at a substrate temperature of 200 °C using SR ablation of PTFE, PFA, and FEP targets.

rate in the case of FEP film was due to the larger quantity of fragments generated by the SR ablation of FEP than those in the cases of PFA and PTFE.

Figure 12 shows the FTIR spectra of the film deposited using the SR ablation of PTFE, PFA, and FEP at the dose of 50 min mA and the substrate temperature of 200 °C. As shown in Fig. 12, relatively strong twin peaks at 1200 and 1141 cm^{-1} corresponding to CF_2 asymmetrical stretching and symmetrical stretching modes, respectively, appeared in the absorption spectra of the deposited films. Additionally, the weak peak of CF_2 wagging mode appeared at 635 cm^{-1} . Features of the FTIR spectra of the deposited films were similar to those of Teflon targets for the most part. However, the weak peak of CF_3 stretching mode appeared at 981 cm^{-1} in all spectra of the deposited films. As summarized in Table

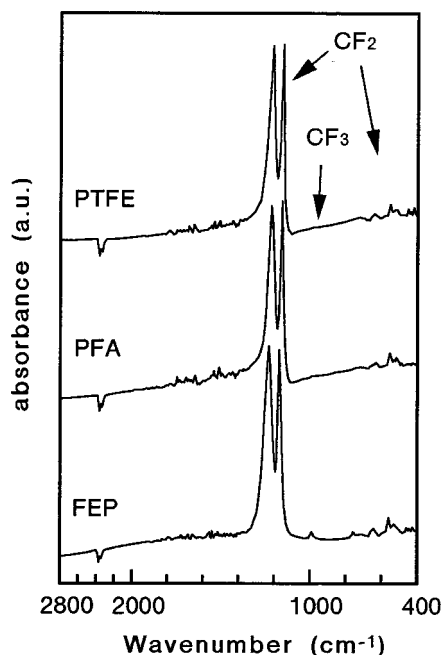


FIG. 12. FTIR spectra of films deposited using SR ablation of PTFE, PFA, and FEP at a dose of 50 min mA and a substrate temperature of 200 °C.

TABLE II. Area of CF , CF_2 , and CF_3 components in targets and the deposited films measured from XPS C (1s) spectra. The total area of C (1s) spectrum was normalized to 100 for each sample.

Material	CF	CF_2	CF_3
PTFE			
Target	0	100	0
Deposited films (27 °C)	4.7	86.2	9.1
Deposited films (200 °C)	4.6	87.1	8.3
FEP			
Target	0	95.2	4.8
Deposited films (27 °C)	6.0	84.1	9.9
Deposited films (200 °C)	5.2	85.4	9.4
PFA			
Target	0	100	0
Deposited films (27 °C)	5.4	86.3	8.3
Deposited films (200 °C)	4.8	87.8	7.4

I, the CF_3 component is not contained in the chemical structure of PTFE, while PFA and FEP contain the CF_3 component. Therefore, the chemical structure of the film deposited by the SR ablation of PTFE was somewhat different from that of the PTFE target. The chemical structures of targets and deposited films were investigated by XPS. Table II summarizes the areas of CF , CF_2 , and CF_3 components in targets and the deposited films measured from XPS carbon (C) (1s) spectra. The total area of C (1s) spectrum was normalized to 100 for each sample. As summarized in Table II, the films formed from all targets contained CF and CF_3 components as well as CF_2 component, and the $\text{CF}/\text{CF}_2/\text{CF}_3$ ratio for each deposited film was almost 5/86/9. Since the CF_3 component was larger than CF component, the F/C ratio of the deposited films was 2–2.1. Moreover, the $\text{CF}/\text{CF}_2/\text{CF}_3$ ratio of the deposited films did not change with varying the substrate temperature. These facts indicate that the fragments containing CF and CF_3 components were generated from Teflon targets irradiated by the SR beam. From these results, the CF_2 -rich polymer containing a small amount of CF and CF_3 components was found to be formed at high rate by Teflon ablation using SR.

As shown in Figs. 8–10, Teflon films with smooth surface and high density were successfully formed by the SR ablation process at the substrate temperature above 200 °C. As a demonstration of the completely dry process employing SR, micromachining of Teflon films formed by using SR ablation was carried out. Figure 13 shows the SEM image of the SR-ablated pattern created in a Teflon film which was formed by the SR ablation of FEP at the substrate temperature of 200 °C. As seen in Fig. 13, the fine pattern with 77 μm square holes was successfully created in the deposited Teflon film by the irradiation of SR beam. It should be noted that the SR ablation process potentially enables us to form the Teflon film onto the curved surface as well as to micro-machine the Teflon film covering the curved substance. Therefore, the SR ablation process can be successfully applied to the fabrication of Teflon microparts in a micromachine.

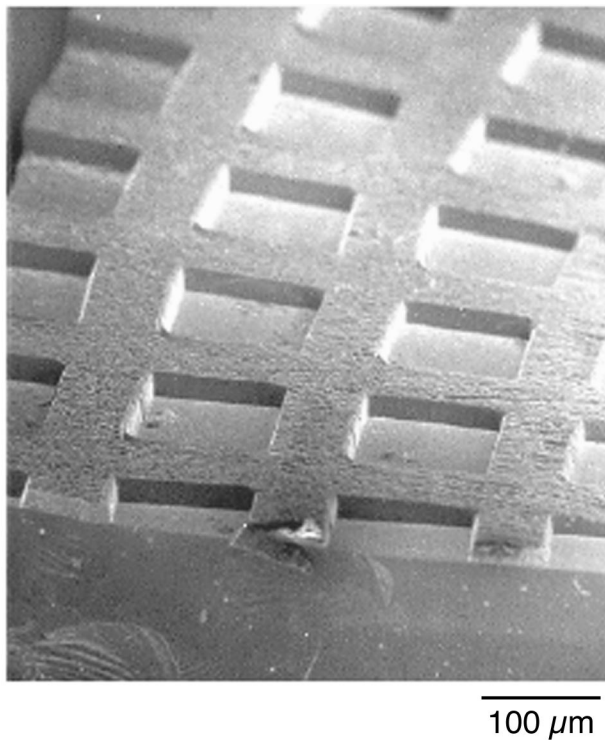


FIG. 13. SEM photograph of SR-ablated pattern created in Teflon film formed at a substrate temperature of 200 °C by SR ablation of FEP.

The SR ablation process would be applicable to the micromachining of metal microparts as well. Figure 14 shows a schematic diagram of the procedure for the fabrication of metal microparts as an example of the application of the SR ablation process. This procedure consists of (a) Teflon film coverage on the surface of a metal material in micron size using the SR ablation, (b) micromachining of Teflon film using the SR ablation, (c) electric plating, and (d) removal of Teflon film. Metal microparts with complicated structure would be realized by using this procedure shown in Fig. 14.

IV. CONCLUSION

The feasibility of the completely dry process using the SR ablation for the direct micromachining and film formation of Teflon was demonstrated. The anisotropic micromachining and thin film formation of PTFE, FEP, and PFA were demonstrated using the SR ablation process. The anisotropic micromachining of Teflon with hole pattern of 2 μm diam was successfully performed, and the micromachining of Teflon with a high aspect ratio of 50 was achieved. The ablation rate of FEP, which has the lowest molecular weight and melting temperature among three kinds of Teflon materials investigated, was higher than those of PFA and PTFE. Moreover, the formation of Teflon films was achieved by the SR ablation process. The Teflon films with flat surface were formed at the substrate temperature above 200 °C. The deposition rate of film formed by the SR ablation of FEP was higher

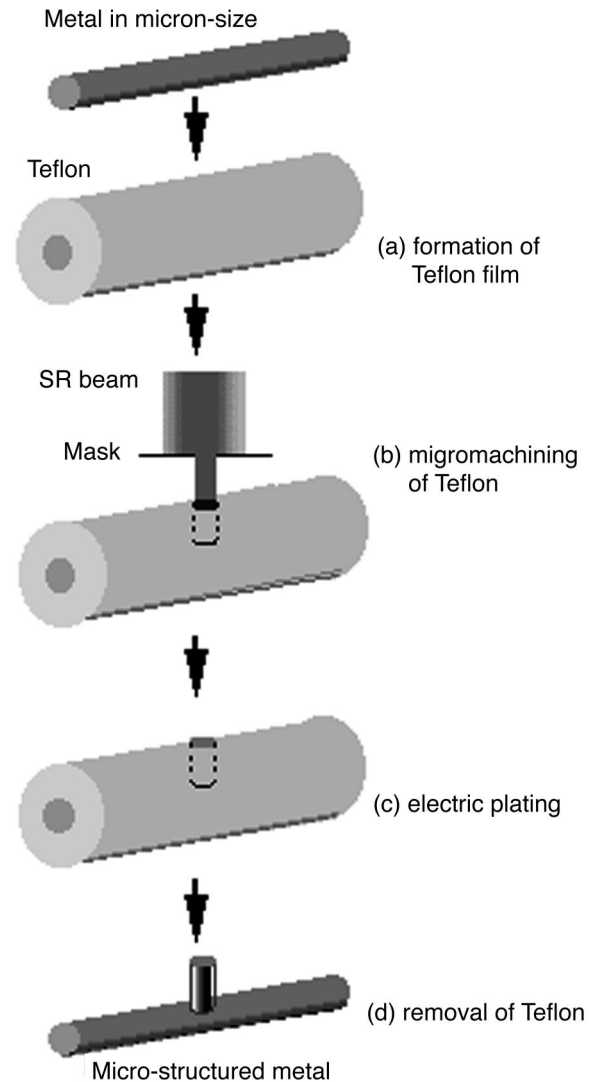


FIG. 14. Schematic diagram of the procedure for the fabrication of metal microparts using the SR ablation process. This procedure consists of (a) Teflon film formation on the curved surface of a metal substance in micron size using the SR ablation, (b) micromachining of Teflon film using the SR ablation, (c) electric plating, and (d) removal of Teflon film.

than those for the cases of PFA and PTFE. It was indicated that the SR ablation process has a possibility of replacing the LIGA process.

ACKNOWLEDGMENTS

This work was supported by the Joint Studies Program (1996–1997) of the Institute for Molecular Science, Okazaki National Research Institute, Japan. The authors thank the Instrument Center, the Institute for Molecular Science, for the use of SEM (Hitachi S-900).

¹S. Kuper and M. Stuke, *Appl. Phys. Lett.* **54**, 4 (1989); G. B. Blanchet and S. Ismat Shah, *ibid.* **62**, 1026 (1993).

²R. Srinivasan and B. Braren, *Chem. Rev.* **89**, 1850 (1994).

³H. Kumagai, K. Midorikawa, K. Toyoda, S. Nakamura, T. Okamoto, and M. Obara, *Appl. Phys. Lett.* **65**, 1850 (1994).

⁴E. W. Becker, W. Ehrfeld, P. Gabmann, A. Maner, and D. Munchmeyer,

- Microelectron. Eng. **4**, 35 (1986); R. A. Rosenberg, S. P. Frigo, and J. K. Simons, Appl. Surf. Sci. **79/80**, 47 (1994); A. W. Wilson, Solid State Technol. **29**, 249 (1986); M. Hori, T. Yoneda, S. Morita, and S. Hattori, J. Electrochem. Soc. **134**, 707 (1987).
- ⁵Y. Zhang, T. Katoh, M. Washino, H. Yamada, and S. Hamada, Appl. Phys. Lett. **67**, 872 (1995); T. Katoh and Y. Zhang, *ibid.* **68**, 865 (1996); Y. Zhang and T. Katoh, Jpn. J. Appl. Phys., Part 2 **35**, L186 (1996).
- ⁶M. Inayoshi, M. Ikeda, M. Hori, Y. Goto, M. Hiramatsu, and A. Hiraya, Jpn. J. Appl. Phys., Part 2 **34**, L1675 (1995).
- ⁷A. Tanaka, J. Electron Microsc. **43**, 177 (1994).